Structural and Functional Characterization of the Alanine Racemase from

Streptomyces coelicolor A3(2)

Raffaella Tassoni[1*], van der Aart, L.T.[2*], Ubbink, M.[1], Van Wezel, G. P.[2], Pannu, N. S.[1#]

5

1 Leiden Institute of Chemistry, Leiden University, Gorlaeus Laboratories, Eisteinweg 55, 2333 CC Leiden, The Netherlands

2 Microbial Biotechnology and Health, Institute of Biology Leiden, Leiden University, Sylviusweg 72, 2333 BE Leiden, The Netherlands

10   * These authors contributed equally to the work

Corresponding authors:

Navraj S. Pannu: raj@chem.leidenuniv.nl

Gilles P. van Wezel: g.wezel@biology.leidenuniv.nl

15   Marcellus Ubbink: m.ubbink@chem.leidenuniv.nl

Abstract

The conversion of L-alanine (L-Ala) into D-alanine (D-Ala) in bacteria is performed by
pyridoxal phosphate-dependent enzymes called alanine racemases. D-Ala is an essential
component of the bacterial peptidoglycan and hence required for survival. The Gram-positive
bacterium *Streptomyces coelicolor* has at least one alanine racemase encoded by *alr*. Here,
we describe an *alr* deletion mutant of *S. coelicolor* which depends on D-Ala for growth and
shows increased sensitivity to the antibiotic D-cycloserine (DCS). The crystal structure of the
alanine racemase (Alr) was solved with and without the inhibitors DCS or propionate. The
crystal structures revealed that Alr is a homodimer with residues from both monomers
contributing to the active site. The dimeric state of the enzyme in solution was confirmed by
gel filtration chromatography, with and without L-Ala or D-cycloserine. Specificity of the
enzyme was 66 +/- 3 U mg^{-1} for the racemization of L- to D-Ala, and 104 +/- 7 U mg^{-1} for the
opposite direction. Comparison of Alr from *S. coelicolor* with orthologous enzymes from other
bacteria, including the closely related D-cycloserine-resistant Alr from *S. lavendulae*, strongly
suggests that structural features such as the hinge angle or the surface area between the
monomers do not contribute to D-cycloserine resistance, and the molecular basis for
resistance therefore remains elusive.

2

INTRODUCTION

40   All canonical, proteinogenic amino acids, with the exception of glycine, have a stereocenter at the Cα and can exist either as the L- or D-enantiomer. While in the past it was generally accepted that only L-amino acids had a role in living organisms, studies revealed a variety of roles for free D-amino acids, for example in the regulation of bacterial spore germination and peptidoglycan structure [1]. Peptidoglycan is essential for cell shape and osmotic regulation

45   and its biosynthesis is dependent on the availability of the less naturally abundant D-alanine [2-4]. D-alanine (D-Ala) is generated through racemization of the abundant L-enantiomer (L-Ala) by the enzyme alanine racemase [5].

Alanine racemases (Alr; E.C. 5.1.1.1) are conserved bacterial enzymes that belong to the Fold Type III of pyridoxal phosphate (PLP)-dependent enzymes. Crystallographic studies of

50   Alr's from different bacterial species revealed a shared, conserved fold consisting of an eight-stranded α/β barrel at the *N*-terminal domain and a second, *C*-terminal domain mainly consisting of β-sheets. The PLP cofactor is bound to a very conserved lysine residue at the *N*-terminal side of the last helix of the barrel. In all studies, Alr's crystals consist of homo-dimers, with residues from both monomers participating in the formation of the active site.

55   Nevertheless, in-solution studies indicated an equilibrium between monomeric and homo-dimeric states in solution, with the homo-dimer being the catalytically active form [6, 7].

Streptomyces coelicolor is the most widely studied member of the Streptomycetes, which are Gram-positive bacteria with a multicellular mycelial life style that reproduce via sporulation [8]. They are of great importance for medicine and biotechnology, accounting for over half of

60   all antibiotics, as well as for many anticancer agents and immunosuppressants available on the market [9, 10]. Here we describe the heterologous expression, purification and crystal structure of *S. coelicolor* Alr, encoded by *alr* (SCO4745). An *alr* null mutant of *S. coelicolor* depends on exogenous D-Ala for growth. The purified enzyme catalyzed the racemization of L-Ala to D-Ala *in vitro* and was shown to be a dimer from gel filtration, both in the absence

65   and presence of L-Ala or the inhibitor D-cycloserine (DCS). Furthermore, the crystal structure of the enzyme has been solved both in the absence and in the presence of the inhibitors

3

DCS and propionate. The comparison of the Alr enzymes from *S. coelicolor* and its close relative the DCS-resistant *Streptomyces lavendulae* [11] questions the structural role of Alr in DCS resistance.

70

MATERIALS AND METHODS

Bacterial strains and culturing conditions

Escherichia coli strains JM109 [12] and ET12567 [13] were used for routine cloning procedures and for extracting non-methylated DNA, respectively. *E. coli* BL21 Star

75 (DE3)pLysS was used for protein production. Cells of *E. coli* were incubated in lysogenic broth (LB) at 37°C. *Streptomyces coelicolor* A3(2) M145 was obtaime from the John Innes cenre strin collection and was the parent of all mutants in this work. All media and routine *Streptomyces* techniques have been described in the *Streptomyces* laboratory manual [13]. Soy, flour and mannitol (SFM) agar plates were used for propagating *S. coelicolor* strains

80 and for preparing spore suspensions. Solid minimal medium (MM) agar plates supplied with 1% (w/v) mannitol was used for phenotypic characterization. The MIC for D-cycloserine was measured in triplicate in 96 well plates containing solid MM, D-alanine and D-cycloserine. Growth was assayed after two days using a resazurin-assay [14].

85 ### *Streptomyces coelicolor* knock-out mutant and genetic complementation

S. coelicolor alr deletion mutants were constructed as previously described [15]. The -1238/-3 and +1167/+2378 regions relative to the start of *alr* were amplified by PCR using primer alr_LF and alr_LR, and alr_RF and alr_RR (Table S2) as described [16]. The left and right flanks were cloned into the unstable, multi-copy vector pWHM3 (Table S1) [17], to allow for

90 efficient gene disruption [18]. The apramycin resistance cassette *aac(3)IV* flanked by *loxP* sites was cloned into the engineered XbaI site to create knock-out construct pGWS1151. Media were supplemented with 1 mM D-Ala to allow growth of *alr* mutants. The correct recombination event in the mutant was confirmed by PCR. For genetic complementation, the -575/+1197 region (numbering relative to the *alr* translational start codon) encompassing the

4

95   promoter and coding region of SCO4745 was amplified from the *S. coelicolor* M145 chromosome using primer 4745FW-575 and 4745RV+1197 (Table S2) and cloned into pHJL401 [19]. pHJL401 is a low-copy number shuttle vector that is very well suited for genetic complementation experiments [20].

100   **Cloning, protein expression and purification**

The *alr* gene (SCO4745) was PCR-amplified from genomic DNA of *Streptomyces coelicolor* using primers alr-FW and alr-RV (Table S2), and cloned into pET-15b with a *N*-terminal His$_6$ tag. The construct was transformed into *E. coli* BL21 Star (DE3)pLysS electrocompetent cells (Novagen). *E. coli* cultures were incubated in LB medium at 37°C until an OD$_{600}$ of 0.6 and

105   gene expression induced by adding 0.5 mM isopropyl β-D-1-thiogalactopyranoside (IPTG) followed by overnight incubation at 16°C. His$_6$-tagged Alr was purified using a pre-packed HisTrap FF column (GE Healthcare) as described [21]. Briefly, after binding of the protein, the column was washed with ten column volumes of 20 mM sodium phosphate buffer, pH 7.0, 500 mM NaCl and 50 mM imidazole and *N*-terminally His$_6$-tagged Alr eluted with the

110   same buffer but containing 250 mM imidazole. Fractions containing the Alr were deslated using a PD-10 column (GE Healthcare) to remove the imidazole and Alr purified further by gel-filtration using a Superose-12 column (GE Healthcare). The collected fractions were analyzed by SDS-PAGE and those containing pure Alr were pooled, concentrated using a Centriprep centrifugal filter unit (10 kDa cut-off, Millipore), and flash-frozen in liquid nitrogen.

115

Enzymatic assay for recombinant Alr

0.2 nM purified Alr was added to 10 mM L-Ala in 20 mM PBS buffer, pH 7.0 and incubated at room temperature (21°C) for 0, 1, 5, 15, 30, and 60 min. The reaction was stopped by heat inactivation for 3 min at 95°C. As a control, 0.2 nM heat-inactivated Alr was used. A 20-µL

120   aliquot of the reaction mixture was added to a 2-mL well in a 24-well plate containing solid MM, inoculated with the *alr* mutant. 0, 10 µM, 50 µM 100 µM, 500 µM and 1 mM D- and L-Ala were added as controls.

Mass spectrometry analysis

125   The identity of the heterologous Alr was verified by mass spectrometry of the tryptic digest. Five µg of purified Alr were denatured in 50 µL 8 M urea in 100 mM NH_4HCO_3. The cysteine residues were reduced with 5 µL of 5 mM dithiothreitol (DTT) for 15 min at 50°C alkylated with 10 µL of 10 mM iodoacetamide at room temperature in the dark for 30 min. The protein was digested overnight at 37°C using 50 ng of modified porcine trypsin (Promega) in 350 µL

130   of 20 mM NH_4HCO_3. The tryptic digest was desalted using stage tips [22], dried and resuspended in 50 µL of H₂O:ACN:FA (96.9:3:0.1) solution. The LTQ-Orbitrap (Thermo Fisher Scientific, Waltham, MA) tandem mass spectrometry analysis was performed as previously described [22].

135   **Crystallization conditions and data collection**

Purified Alr was concentrated to 20 mg mL^{-1} and crystallization conditions were screened by sitting-drop vapor-diffusion using the JCSG+ and PACT *premier* (Molecular Dimensions) screens at 20°C with 500-nL drops. The reservoir (75 µL) was pipetted by a Genesis RS200 robot (Tecan). Drops were made by an Oryx6 robot (Douglas Instruments). After 1 day,

140   crystals grew in condition number 2-38 of PACT *premier*, which consisted of 0.1 M BIS-TRIS propane, pH 8.5, 0.2 M NaBr, 20% (w/v) PEG3350. Bigger crystals were grown in 1-µL drops. Prior to flash-cooling in liquid nitrogen, crystals were soaked in a cryosolution consisting of mother liquor, 10% glycerol and 10, 5, or 1 mM inhibitor to obtain the DCS- and propionate-bound structures.

145   X-ray data collection was performed at the ESRF (Grenoble, France) on beamline ID23-1 [23] using a PIXEL, Pilatus_6M_F X-ray detector. A total of 1127 frames were collected for the native Alr, with an oscillation of 0.15°, an exposure time of 0.378 s, total 426.006 s. The data set was processed by XDS [23] and scaled by AIMLESS [24] to a resolution of 2.8 Å. For the DCS-bound Alr 960 frames were collected, with an oscillation range of 0.15°, an

6

150 exposure time of 0.071 s per image and a total time of 68.16 s. For the propionate-bound

structure, 1240 images were collected, with an oscillation degree of 0.1°, an exposure time

per image of 0.037 s, and a total time of 45.88 s. Both inhibitor-bound data sets were auto-

processed by the EDNA Autoprocessing package in the mxCuBE [25] to a resolution of

1.64 Å and 1.51 Å for the DCS-bound and propionate-bound Alr, respectively. The structures

155 were solved by molecular replacement with *MOLREP* [26] using 1VFH as a search model

from the *CCP4* suite [27] and iteratively refined with REFMAC [28]. Manual model building

was done using *Coot* [29].

Enzyme kinetics

160 The racemization activity of Alr was determined by quantifying the derivatization product of L-

and D-Ala by HPLC, as previously described [30, 31]. The derivatization reagent consisted of

a methanol solution of 10 mg mL^{-1} *o*-phthalaldehyde (OPA, Sigma-Aldrich) and 10 mg mL^{-1}

Boc-L-Cys (Sigma-Aldrich). A 0.4 M boric acid solution was adjusted to pH 9.0 with sodium

hydroxide. The reaction mixture consisted of 20 µL of 20 mM sodium phosphate buffer, pH

165 7.0 containing varying amounts of L- or D-Ala from 281 µM to 20 mM. The reaction was

started by adding 100 nM of enzyme and stopped after 10 min at 25°C by adding 20 µL of

2 N HCl. The reaction mixture was neutralized by NaOH. After adding 350 µL of boric acid

buffer and 100 µL of derivatization reagent, derivatization was conducted for 5 min at 25°C.

The fluorescent products were separated on a Kinetex EVO C18 column (Phenomenex) by a

170 gradient from 24% to 46.75% of acetonitrile in water in 30 min and detected by a Shimadzu

RF-10AXL fluorescence detector.

RESULTS AND DISCUSSION

175 **Creation of an *alr* null mutant of *S. coelicolor***

To study the role of *alr* in amino acid metabolism and in morphogenesis of *S. coelicolor*, a deletion mutant was created by removal of the entire coding region (see Materials & Methods). In line with its expected role in biosynthesis of the essential D-amino acid D-Ala, *alr* null mutants depended on exogenously added D-Ala (50 μM) for growth (Fig 1a). Re-

180 introducing a copy of the *alr* gene via plasmid pGWS1151 complemented the mutant phenotype, allowing growth in the absence of added D-Ala (Fig 1a). These data show that *alr* encodes alanine racemase in *S. coelicolor*, and that it most likely is the only gene encoding this enzyme.

185 **Alr is the only alanine racemase in *S. coelicolor***

The Alr from *S. coelicolor* (Alr$_{Sco}$) shares 74.9% aa sequence identity with the Alr from the DCS-producing *Streptomyces lavendulae* (Alr$_{Sla}$) [11] and 37.9% with the well-studied Alr from *Geobacillus stearothermophilus* (Alr$_{Gst}$) [32] (Fig. 2). To analyze the activity and kinetics of the enzyme, recombinant His$_6$-tagged Alr was expressed in *E. coli* BL21 Star cells and

190 purified to homogenity (see Materials and Methods section). Around 45 mg of pure Alr was obtained from 1 L of bacterial culture and Alr was identified using mass spectrometry (Table S4).

To establish if Alr$_{Sco}$ converts L-Ala into D-Ala, we designed a combined *in vitro* and *in vivo* assay, whereby 10 mM L-Ala was incubated with 0.2 nM purified Alr-His$_6$ for 10 sec to

195 60 min, after which the enzyme was heat-inactivated and the mixture was added to minimal media (MM) agar plates, followed by plating of 10^6 spores of the *alr* null mutant and incubation of 5 days at 30°C (Fig. 1b). If Alr converts L-Ala into D-Ala, the reaction should generate sufficient D-Ala to allow restoration of growth to *alr* null mutants. Indeed, sufficient D-Ala was produced to allow growth of the *alr* null mutant, whereby biomass accumulaiton

200 was proportional to the incubation time, while a control experiment with extracts from heat-inactivated Alr did not give any growth (Fig. 1b). Addition of D-Ala also restored growth of *alr*

8

mutants, while no growth was seen for cultures grown in the presence of added L-Ala. Taken together, this shows that no Alr activity is present in *S. coelicolor alr* mutants, and that Alr actively converts L-Ala into D-Ala *in vitro*.

205   The kinetic parameters of recombinant Alr_{Sco} were determined using both L- and D-Ala as substrates. The enzyme shows a K_m of 6.3 mM and 8.9 mM towards L- and D-Ala, respectively (Table 1). For comparison, kinetic parameters of Alr_{Sla} [11] and Alr_{Gst} are also shown in Table 1.

To analyze possible multimerization of Alr_{Sco}, analytical gel filtration was used, which

210   established an apparent molecular weight for the protein of 83 kDa in solution both in the absence and in the presence of L-Ala and DCS (Figure S2); this corresponds roughly to two Alr proteins (43.4 kDa per subunit). See Supplementary Data for more details. These data suggest that Alr_{Sco} forms a dimer in solution, both in the presence and in the absence of ligands.

215

Overall structure of Alr from *Streptomyces coelicolor*

The crystal structure of ligand-free Alr_{Sco} was determined to a resolution of 2.8 Å (Table 2). The overall structure is similar to that of other prokaryotic Alr proteins [11, 33]. The asymmetric unit contains four protein molecules (A-D), which interact in a head-to-tail

220   manner to form two dimers (dimer A-B and C-D, Fig. 3a). Each monomer has two structurally distinct domains. The *N*-terminal domain, comprising residues 1-259, has an eight-stranded α/β-barrel fold, typical of phosphate-binding proteins. The *C*-terminal domain, residues 260-391, contains mostly β-strands (Fig. 3b). 96% of the amino acids are in the preferred regions of the Ramachandran plot, 4% are in the allowed regions and no residues are in the

225   unfavored areas. After refinement, the r.m.s. deviation between Cα's of the two interacting molecules A and B is 0.0794 Å, and between C and D is 0.1431 Å.

There are two active sites per dimer, which are located at the interface between each α/β-barrel of one subunit and the *C*-terminal domain of the other. The catalytic core (Fig. 4a) consists of the PLP cofactor, a Lys, and a Tyr, which is contributed by the other subunit. The

9

230 PLP is bound through an internal aldimine bond to the amino group of Lys46, located at the *C*-terminal side of the first β-strand of the α/β-barrel. The side chain of the catalytic Lys46 points out of the α/β-barrel, towards the *C*-terminal domain of the interacting subunit, and in particular, towards Tyr283'. The phosphate group of the PLP is stabilized by hydrogen bonds with the side chains of Tyr50, Ser222 and Tyr374, and with the backbone of Gly239, Ser222

235 and Ile240. The pyridine ring of the PLP is stabilized by a hydrogen bond between the N-1 of the cofactor and Nε of Arg237. The C2A of the PLP also interacts with oxygen Q1 of the carboxylated Lys141. All residues stabilizing the PLP cofactor (Tyr50, Ser222, Gly239, Ile240, Arg237, Tyr374) are conserved among Alr's [32]. However, the Alr_{Sco} lacks one important hydrogen bond between Arg148 and the phenolic oxygen of the PLP molecule, as

240 already observed for the Alr_{Sla} [34] [35]. Among the residues involved in PLP-stabilization, Tyr374, which corresponds to Tyr354 in the well-studied Alr_{Gst}, is particularly interesting. In fact, while always regarded as a PLP-stabilizer, Tyr354 was shown to be actually anchored by the hydrogen bond with the PLP so to ensure substrate specificity of the Alr [36].

245 **Alr crystal structures bound to propionate and DCS**

The structure of Alr_{Sco} was solved in the presence of the two inhibitors propionate [37] and DCS [11] to a resolution of 1.51 Å and 1.64 Å, respectively. In Alr_{Sco}, the carboxylic group of propionate binds in the same orientation in all four active sites present in the crystal unit. One of the carboxylic oxygens of propionate forms hydrogen bonds with the amino group of

250 Met331', the phenolic oxygen and CE2 of Tyr283' and a water molecule, which bridges the substrate to several other water molecules in the active site. The second carboxylic oxygen of propionate interacts with Nζ of Lys46, C4A of PLP, the phenolic oxygen of Tyr283' and a water molecule. The electron density around C3 of propionate shows that this atom can have several orientations in the active site. In fact, it can either interact with O4 of the phosphate of

255 PLP, the phenolic oxygen of Tyr283' and a water molecule, or with the phenolic oxygen of Tyr50, the CE of Met331', Nζ of Lys46 and C4A of PLP (Fig. 4b). Both in Alr_{Sco} and Alr_{Gst} the hydrogen-bonding network stabilizing the propionate is very conserved. As argued by [37],

10

the propionate-bound form of the Alr can be considered a mimic of the Michaelis complex formed between the enzyme and its natural substrate L-Ala.

260   DCS is an antibiotic produced by *S. lavendulae* and *Streptomyces garyphalus*, which covalently inhibits Alr [11, 38-42]. The structure of the Alr$_{Sco}$ in complex with DCS shows that the amino group of the inhibitor replaces the Lys46 in forming a covalent bond with the PLP C4 (Fig. 4c). The nitrogen and oxygen atoms in the isoxazole ring form hydrogen bonds with Tyr302', Met331' and a water molecule. The hydroxyl group of the DCS ring also interacts

265   with Met331' and Arg148 (Fig. 4c). The catalytic Tyr283' is at hydrogen-bond distance from the amino group of DCS. DCS molecules superpose well in three of the active sites of the crystal (A, B and C). However, the DCS-PMP adduct in the fourth site showed a shift of the DCS compared to the other sites, while PLP still superposed well. Comparison of the hydrogen bonds in the proximity of the active site in the free and in the DCS-bound form of

270   Alr, revealed a role for Arg148 in substrate stabilization. In fact, while the side chain of Arg148 is hydrogen-bonded to Gln333 in free Alr, it shifted towards the hydroxyl moiety of the DCS upon binding of the inhibitor. Gln333 was stabilized by interaction with carboxylated Lys141. The rearrangement of the hydrogen bonds involving Arg148, Gln333 and Lys141 does not occur in the propionate-bound structure, suggesting that Arg148 is involved in

275   stabilization of the carboxylic group of the substrate.

Alr and DCS resistance

Alr$_{Sco}$ shows high sequence and structural similarity to Alr$_{Sla}$. Based on crystallographic studies, Alr$_{Sla}$ was proposed as one determinant of DCS resistance in the producer strain

280   [11]. However, detailed structural comparison of different Alr proteins based on interatomic distances between active site residues, dimerization areas and hinge angles (see Supplementary Data), failed to establish a clear correlation between structural features and DCS resistance. It therefore remains unclear what the role of Alr is in DCS resistance in the producer strain.

285

11

In conclusion, our work shows that SCO4745 encodes the only Alr in *S. coelicolor* A3(2) and is essential for growth. Our structural studies on Alr_{Sco} and comparison to Alr_{Sla} suggest that there are more factors contributing to DCS resistance in bacteria, which relates well to recent studies on DCS-producing streptomycetes [43] and DCS-resistant strains of *M. tuberculosis*

290   [44-47], . The availability of a *S. coelicolor alr*-null mutant and the crystal structure of the Alr from the same bacterium offer a new, valuable model for the study of DCS resistanc

In conclusion, our work shows that SCO4745 encodes the only Alr in *S. coelicolor* A3(2) and

12

REFERENCES

1. Cava, F., et al., *Emerging knowledge of regulatory roles of d-amino acids in bacteria.* Cellular and Molecular Life Sciences, 2011. **68**(5): p. 817-831.

2. Lam, H., et al., *D-amino acids govern stationary phase cell wall remodeling in bacteria.* Science, 2009. **325**(5947): p. 1552-5.

3. Steen, A., et al., *Autolysis of Lactococcus lactis is increased upon D-alanine depletion of peptidoglycan and lipoteichoic acids.* J Bacteriol, 2005. **187**(1): p. 114-24.

4. Vollmer, W., D. Blanot, and M.A. de Pedro, *Peptidoglycan structure and architecture.* FEMS Microbiol Rev, 2008. **32**(2): p. 149-67.

5. Walsh, C.T., *Enzymes in the D-alanine branch of bacterial cell wall peptidoglycan assembly.* Journal of Biological Chemistry, 1989. **264**(5): p. 2393-2396.

6. Ju, J., et al., *Correlation between catalytic activity and monomer-dimer equilibrium of bacterial alanine racemases.* J Biochem, 2011. **149**: p. 83 - 89.

7. Strych, U., et al., *Purification and preliminary crystallization of alanine racemase from Streptococcus pneumoniae.* BMC Microbiol, 2007. **7**: p. 40.

8. Claessen, D., et al., *Bacterial solutions to multicellularity: a tale of biofilms, filaments and fruiting bodies.* Nat Rev Microbiol, 2014. **12**(2): p. 115-24.

9. Barka, E.A., et al., *Taxonomy, physiology, and natural products of the Actinobacteria.* Microbiol Mol Biol Rev, 2016. **80**(1): p. 1-43.

10. Hopwood, D.A., *Streptomyces in nature and medicine: the antibiotic makers*2007, New York: Oxford University Press.

11. Noda, M., et al., *Structural Evidence That Alanine Racemase from a d-Cycloserine-producing Microorganism Exhibits Resistance to Its Own Product.* Journal of Biological Chemistry, 2004. **279**(44): p. 46153-46161.

12. Sambrook, J., E.F. Fritsch, and T. Maniatis, *Molecular cloning: a laboratory manual.* 2nd ed1989, Cold Spring harbor, N.Y.: Cold Spring Harbor laboratory press.

13. Kieser, T., et al., *Practical Streptomyces genetics*2000, Norwich, U.K.: John Innes Foundation.

14. Mann, C. and J. Markham, *A new method for determining the minimum inhibitory concentration of essential oils.* Journal of Applied Microbiology, 1998. **84**(4): p. 538-544.

15. Swiatek, M.A., et al., *Functional analysis of the N-acetylglucosamine metabolic genes of Streptomyces coelicolor and role in the control of development and antibiotic production.* J Bacteriol, 2012. **194**(5): p. 1136-1144.

16. Colson, S., et al., *Conserved cis-acting elements upstream of genes composing the chitinolytic system of streptomycetes are DasR-responsive elements.* J Mol Microbiol Biotechnol, 2007. **12**(1-2): p. 60-6.

17. Vara, J., et al., *Cloning of genes governing the deoxysugar portion of the erythromycin biosynthesis pathway in Saccharopolyspora erythraea (Streptomyces erythreus).* J Bacteriol, 1989. **171**(11): p. 5872-81.

18. van Wezel, G.P., et al., *GlcP constitutes the major glucose uptake system of Streptomyces coelicolor A3(2).* Mol Microbiol, 2005. **55**(2): p. 624-36.

19. Larson, J.L. and C.L. Hershberger, *The minimal replicon of a streptomycete plasmid produces an ultrahigh level of plasmid DNA.* Plasmid, 1986. **15**(3): p. 199-209.

20. van Wezel, G.P., et al., *Application of redD, the transcriptional activator gene of the undecylprodigiosin biosynthetic pathway, as a reporter for transcriptional activity in Streptomyces coelicolor A3(2) and Streptomyces lividans.* J Mol Microbiol Biotechnol, 2000. **2**(4): p. 551-6.

21. Mahr, K., et al., *Glucose kinase of Streptomyces coelicolor A3(2): large-scale purification and biochemical analysis.* Antonie Van Leeuwenhoek, 2000. **78**(3-4): p. 253-61.

22. Li, N., et al., *Relative quantification of proteasome activity by activity-based protein profiling and LC-MS/MS.* Nat Protoc, 2013. **8**(6): p. 1155-68.

23. Kabsch, W., *Xds.* Acta Crystallogr D Biol Crystallogr, 2010. **66**(Pt 2): p. 125-32.

24. Evans, P.R. and G.N. Murshudov, *How good are my data and what is the resolution?* Acta Crystallogr D Biol Crystallogr, 2013. **69**(Pt 7): p. 1204-14.

25. Gabadinho, J., et al., *MxCuBE: a synchrotron beamline control environment customized for macromolecular crystallography experiments.* J Synchrotron Radiat, 2010. **17**(5): p. 700-7.

26. Vagin, A. and A. Teplyakov, *MOLREP: an Automated Program for Molecular Replacement.* Journal of Applied Crystallography, 1997. **30**(6): p. 1022-1025.

27. Winn, M.D., et al., *Overview of the CCP4 suite and current developments.* Acta Crystallographica Section D: Biological Crystallography, 2011. **67**(Pt 4): p. 235-242.

28. Murshudov, G.N., et al., *REFMAC5 for the refinement of macromolecular crystal structures.* Acta Crystallogr D Biol Crystallogr, 2011. **67**(Pt 4): p. 355-67.

29. Emsley, P. and K. Cowtan, *Coot: model-building tools for molecular graphics.* Acta Crystallographica Section D, 2004. **60**(12 Part 1): p. 2126-2132.

30. Hashimoto, A., et al., *Determination of free amino acid enantiomers in rat brain and serum by high-performance liquid chromatography after derivatization with N-tert.-butyloxycarbonyl-l-cysteine and o-phthaldialdehyde.* Journal of Chromatography B: Biomedical Sciences and Applications, 1992. **582**(1–2): p. 41-48.

31. Ju, J., et al., *Cloning of alanine racemase genes from Pseudomonas fluorescens strains and oligomerization states of gene products expressed in Escherichia coli.* Journal of Bioscience and Bioengineering, 2005. **100**(4): p. 409-417.

32.   Shaw, J., G. Petsko, and D. Ringe, *Determination of the structure of alanine racemase from Bacillus stearothermophilus at 1.9-A resolution.* Biochemistry, 1997. **36**: p. 1329 - 1342.

33.   Shaw, J.P., G.A. Petsko, and D. Ringe, *Determination of the Structure of Alanine Racemase from Bacillus stearothermophilus at 1.9-Å Resolution.* Biochemistry, 1997. **36**(6): p. 1329-1342.

34.   Noda, M., et al., *Self-protection mechanism in D-cycloserine-producing Streptomyces lavendulae. Gene cloning, characterization, and kinetics of its alanine racemase and D-alanyl-D-alanine ligase, which are target enzymes of D-cycloserine.* J Biol Chem, 2004. **279**(44): p. 46143-52.

35.   Noda, M., et al., *Structural evidence that alanine racemase from a D-cycloserine-producing microorganism exhibits resistance to its own product.* J Biol Chem, 2004. **279**(44): p. 46153-61.

36.   Patrick, W., J. Weisner, and J. Blackburn, *Site-directed mutagenesis of Tyr354 in Geobacillus stearothermophilus alanine racemase identifies a role in controlling substrate specificity and a possible role in the evolution of antibiotic resistance.* Chembiochem, 2002. **3**: p. 789 - 792.

37.   Morollo, A., G. Petsko, and D. Ringe, *Structure of a Michaelis complex analogue: propionate binds in the substrate carboxylate site of alanine racemase.* Biochemistry, 1999. **38**: p. 3293 - 3301.

38.   Fenn, T.D., et al., *A Side Reaction of Alanine Racemase: Transamination of Cycloserine†,‡.* Biochemistry, 2003. **42**(19): p. 5775-5783.

39.   Asojo, O.A., et al., *Structural and biochemical analyses of alanine racemase from the multidrug-resistant Clostridium difficile strain 630.* Acta Crystallographica Section D: Biological Crystallography, 2014. **70**(Pt 7): p. 1922-1933.

40.   Priyadarshi, A., et al., *Structural insights into the alanine racemase from Enterococcus faecalis.* Biochim Biophys Acta, 2009. **1794**: p. 1030 - 1040.

41.   Wu, D., et al., *Residues Asp164 and Glu165 at the substrate entryway function potently in substrate orientation of alanine racemase from E. coli: Enzymatic characterization with crystal structure analysis.* Protein Sci, 2008. **17**: p. 1066 - 1076.

42.   Lambert, M.P. and F.C. Neuhaus, *Mechanism of d-Cycloserine Action: Alanine Racemase from Escherichia coli W.* Journal of Bacteriology, 1972. **110**(3): p. 978-987.

43.   Matsuo, H., et al., *Molecular cloning of a D-cycloserine resistance gene from D-cycloserine-producing Streptomyces garyphalus.* J Antibiot (Tokyo), 2003. **56**(9): p. 762-7.

44.   Desjardins, C.A., et al., *Genomic and functional analyses of Mycobacterium tuberculosis strains implicate ald in D-cycloserine resistance.* Nat Genet, 2016. **48**(5): p. 544-51.

45.   Hong, W., L. Chen, and J. Xie, *Molecular basis underlying Mycobacterium tuberculosis D-cycloserine resistance. Is there a role for ubiquinone and menaquinone metabolic pathways?* Expert Opin Ther Targets, 2014. **18**(6): p. 691-701.

46.   Feng, Z. and R.G. Barletta, *Roles of Mycobacterium smegmatis D-alanine:D-alanine ligase and D-alanine racemase in the mechanisms of action of and resistance to the peptidoglycan inhibitor D-cycloserine.* Antimicrob Agents Chemother, 2003. **47**(1): p. 283-91.

47.   Chen, J.M., et al., *A point mutation in cycA partially contributes to the D-cycloserine resistance trait of Mycobacterium bovis BCG vaccine strains.* PLoS One, 2012. **7**(8): p. e43467.

48.   Noda, M., et al., *A novel assay method for an amino acid racemase reaction based on circular dichroism.* Biochem J, 2005. **389**: p. 491 - 496.

49.   Kato, S., H. Hemmi, and T. Yoshimura, *Lysine racemase from a lactic acid bacterium, Oenococcus oeni: structural basis of substrate specificity.* Journal of Biochemistry, 2012. **152**(6): p. 505-508.

50.   Inagaki, K., et al., *Thermostable alanine racemase from Bacillus stearothermophilus: molecular cloning of the gene, enzyme purification, and characterization.* Biochemistry, 1986. **25**: p. 3268 - 3274.

Table 1. Kinetic parameters for the racemization of L- and D-Ala by the recombinant Alr.

The Michaelis-Menten constant (K_m), maximum reaction rate (V_{max}) and catalytic constant (k_{cat}) of the Alr from *S. coelicolor* (Alr_{Sco}) are compared to the reported K_m, V_{max} and k_{cat} of the Alr's from *S. lavendulae* (Alr_{Sla}) and *G. stearothermophilus* (Alr_{Gst}).

	L → D			D → L		
	K_m (mM)	V_{max} (U mg^{-1})	k_{cat} (s^{-1})	K_m (mM)	V_{max} (U mg^{-1})	k_{cat} (s^{-1})
Alr_{Sco}	6.3 ± 0.1	66.3 ± 3.3	47.9 ± 2.4	8.9 ± 0.3	104.1 ± 7.8	75.2 ± 5.4
Alr_{Sla}[‡]	0.4 ± 0.1	78.6 ± 4.8[‡‡]	55 ± 3.3	0.4 ± 0.2	90.5 ± 9.5[‡‡]	63.3 ± 6.7
Alr_{Gst}	5.1 ± 0.6[*]	2550[**]	1533.3 ± 50[*]	2.8 ± 0.4[*]	1400[**]	1016.7 ± 33[*]

[‡]Reactions performed at 37°C [48]; [‡‡]Calculated using the published data by [49], and a M_W=42 kDa; [*][49]; [**][50].

Table 2. Data-collection and refinement statistics

	Free Alr	DCS-bound Alr	Propionate-bound Alr
Space group	P 1 21 1	P 1 21 1	P 1 21 1
Unit-cell parameters a, b, c, α, β, γ	78.96, 87.17, 109.63 90.00, 102.26, 90.00	79.74, 88.71, 109.14 90.00, 102.25, 90.00	79.95, 88.58, 108.88 90.00, 102.60, 90.00
Number of observations	116287	480032	532661
Number of unique reflections	34569	177142	224510
Completeness (%)	96.0	77.3	96.6
R_{pim} (%), CC(1/2) highest resolution bin	0.050, 0.991	0.037, 0.997	0.071, 0.985
$\langle I/\sigma(I) \rangle$	1.72	1.38	1.28
Multiplicity	3.4	2.7	2.4
Resolution range (Å)	107.12, 47.78-2.8	106.60(depositor), 49.14(EDS)-1.64	106.26, 48.06-1.51
R factor (%)	21.3	21.6	21.2
R_{free} (%)	26.2	24.5	23.7
R.m.s. deviations			
Bond lengths (Å)	0.62	0.88	0.98
Bond angles (°)	0.84	0.96	1.05
Number of atoms			
Protein (Chains A, B, C, D)	2857, 2833, 2838, 2833	2922, 2851, 2846, 2843	3047, 2911, 2909, 2926
PLP	15	22	15
Water	171	760	804
Ramachandran plot			

(%)			
Preferred regions	96	97	97
Allowed regions	4	3	3
Outliers	0	0	0

FIGURE LEGENDS

Figure 1. SCO4547 encodes alanine racemase Alr.

(A) The *alr* null mutant of *S. coelicolor* requires supplemented D-Ala for growth. This phenotype is rescued by the introduction of plasmid pGWS1151, which expresses Alr. Strains were grown for 5 days on SFM agar plates. (B) Rescue of the *S. coelicolor alr* null mutant with D-Ala produced *in vitro* by Alr. Alr (0.2 nM) was incubated with 10 mM L-Ala for 10 sec or 1, 5, 15, 30 or 60 min, followed by heat inactivation. The reaction mixture was then added to MM agar in 24-well plates and growth of the *alr* null mutant assessed. As a control, the same experiment was done with heat inactivated Alr (Alr*). Note the restoration of growth to the *alr* mutant after addition of the reaction mixture with active Alr, but not with heat-inactivated Alr. The bottom rows show control experiments with added D-Ala or L-Ala (ranging between 0-1 mM).

Figure 2. Multiple aminoacid sequence alignment of the Alr's from *S. coelicolor* (Sco), *S. lavendulae* (Sla; PDB 1VFT) and *G. stearothermophilus* (Gst; PDB 1XQK). The sequence alignment showing structural elements of Alr$_{Sco}$ was generated with ESPript3.0. α-helices are shown as large coils labeled α, 3$_{10}$-helices are shown as small coils labeled η, β-strands are shown as arrows labeled β and β-turns are labeled TT. Identical residues are shown on a red background, conserved residues are shown in red and conserved regions are shown in boxes.

Figure 3. Ribbon representation of the Alr from *S. coelicolor*. (A) The asymmetric unit contains two homo-dimers. The two chains within one dimer are colored in gold and dark cyan. (B) The *N*-terminal domain (1-259) is a α/β-barrel. The *C*-terminal domain (260-391) mostly comprises β-strands. The catalytic Tyr283 is highlighted in red.

20

Figure 4. Active site of the Alr without ligands (A) and in complex with propionate (B) and D-cycloserine (C). The electron density $2F_0$-F_c map is shown for the PLP and the two inhibitors. The residues in the active site which are contributed from the monomer not bound to the PLP are indicated as primed numbers. Dotted lines indicate interatomic distances shorter than 3 Å.

Figure 1

A

M145

Δ*alr*

Δ*alr* +
pGWS1158

M145

Δ*alr*

Δ*alr* +
pGWS1158

+1mM D-Ala

B

	0.2	1	5	15	30	60 min

Alr

Alr*

D-Ala

L-Ala

0	10μM	50μM	100μM	500μM	1mM

Figure 2

Sco   β1   α1   β2   α2   α3
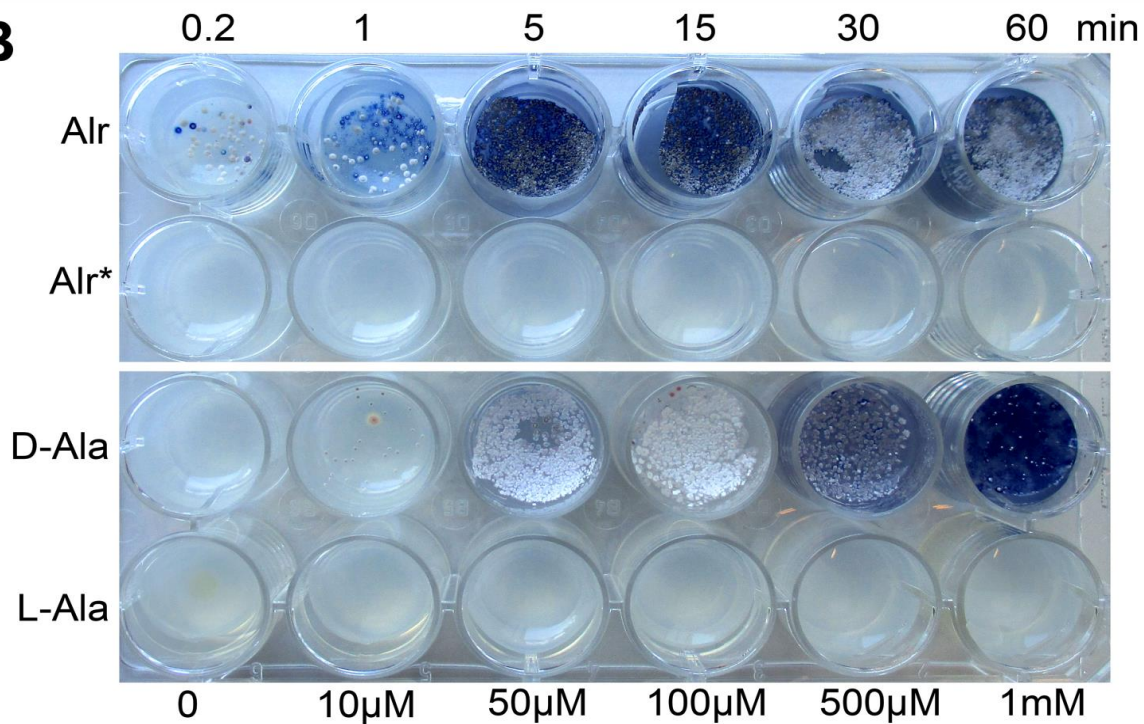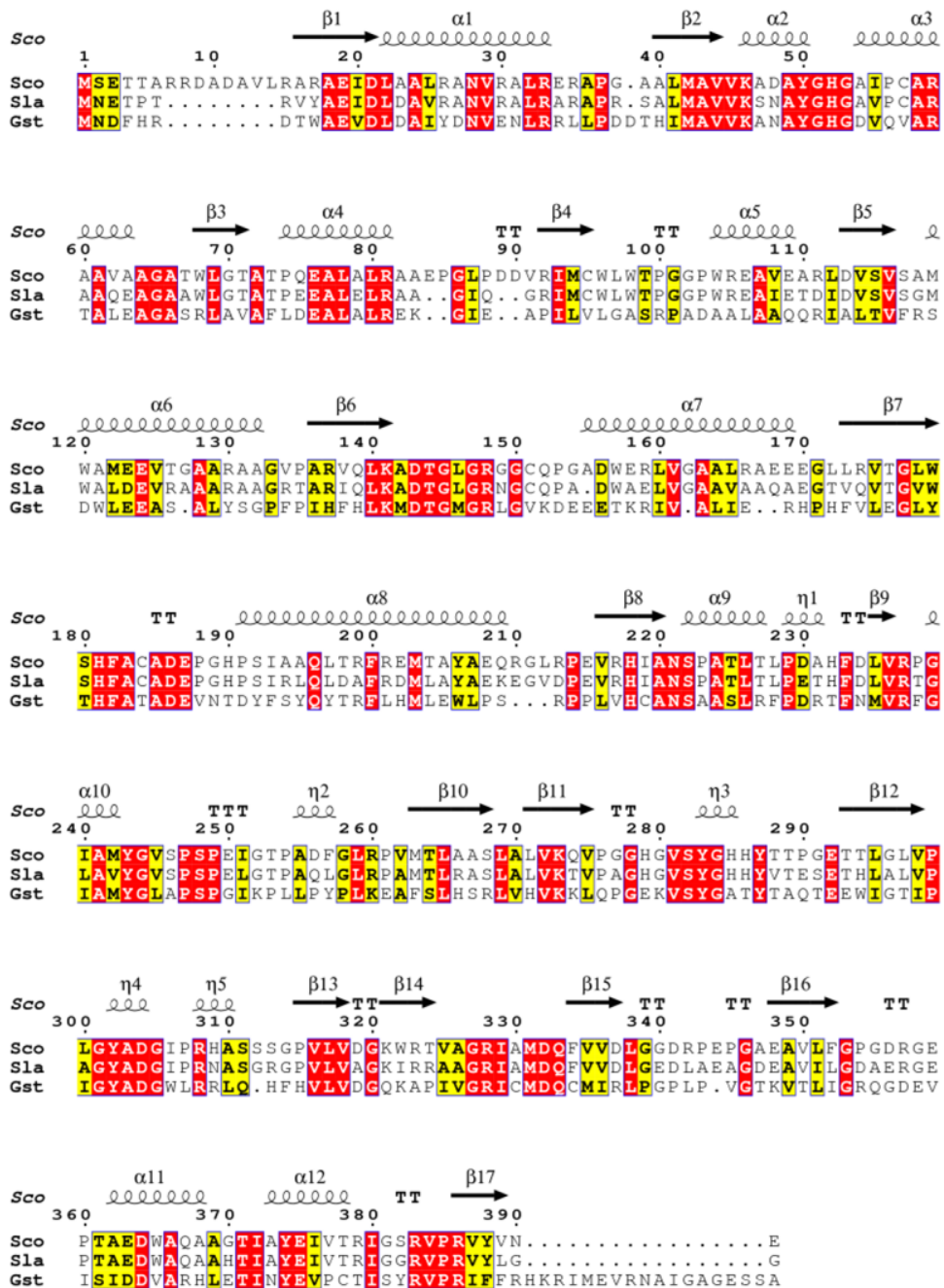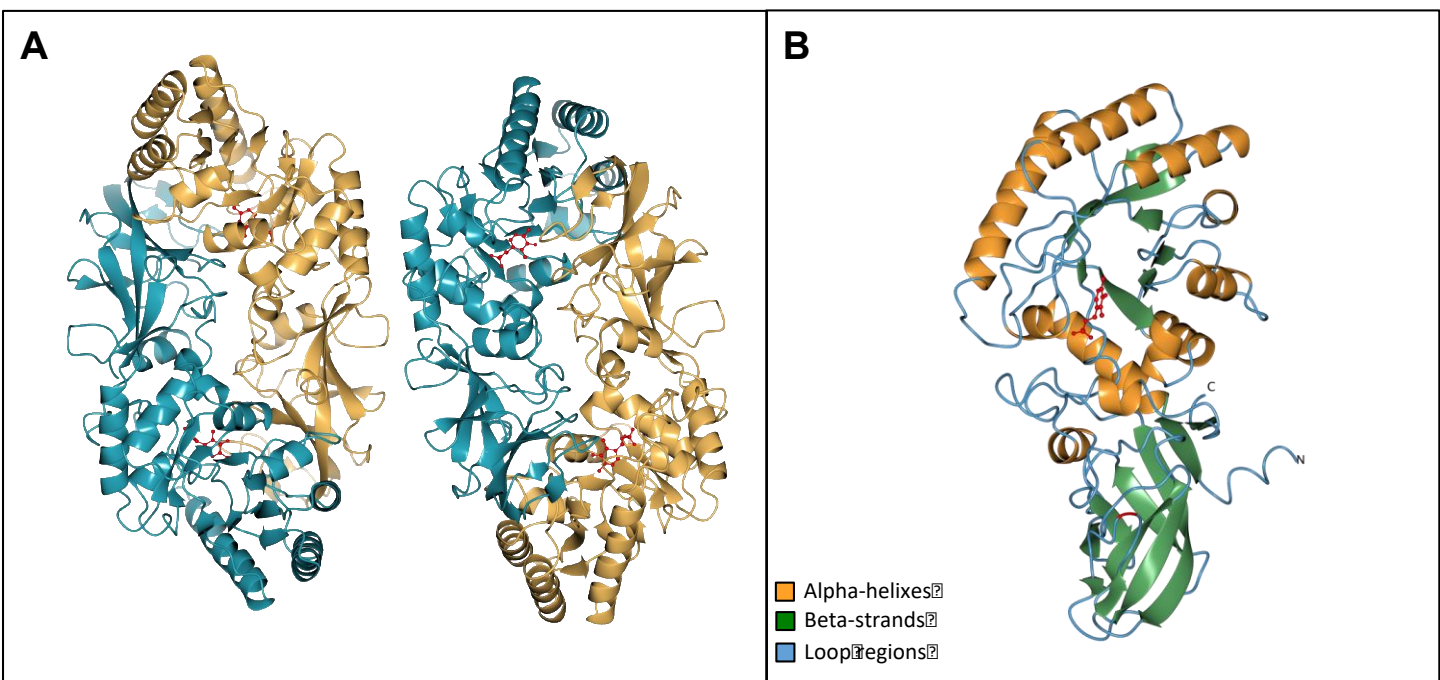
```
        1         10         20         30         40        50
Sco  MSETTARRDADAVLRARAEIDLAALRANVRALRERAPG.AALMAVVKADAYGHGAIPCAR
Sla  MNETPT........RVYAEIDLDAVRANVRALRARAPR.SALMAVVKSNAYGHGAVPCAR
Gst  MNDFHR........DTWAEVDLDAIYDNVENLRRLLPDDTHIMAVVKANAYGHGDVQVAR
```

Sco   β3   α4   TT β4   TT   α5   β5

```
      60        70        80        90       100       110
Sco  AAVAAGATWLGTATPQEALALRAAEPGLPDDVRIMCWLWTPGGPWREAVEARLDVSVSAM
Sla  AAQEAGAAWLGTATPEEALELRAA..GIQ..GRIMCWLWTPGGPWREAIETDIDVSVSGM
Gst  TALEAGASRLAVAFLDEALALREK..GIE..APILVLGASRPADAALAAQQRIALTVFRS
```

Sco   α6   β6   α7   β7

```
      120       130       140       150       160       170
Sco  WAMEEVTGAARAAGVPARVQLKADTGLGRGGCQPGADWERLVGAALRAEEEGLLRVTGLW
Sla  WALDEVRAAARAAGRTARIQLKADTGLGRNGCQPA.DWAELVGAAVAAQAEGTVQVTGVW
Gst  DWLEEAS.ALYSGPFPIHFHLKMDTGMGRLGVKDEEETKRIV.ALIE..RHPHFVLEGLY
```

Sco   TT   α8   β8   α9   η1   β9

```
      180       190       200       210       220       230
Sco  SHFACADEPGHPSIAAQLTRFREMTAYAEQRGLRPEVRHIANSPATLTLPDAHFDLVRPG
Sla  SHFACADEPGHPSIRLQLDAFRDMLAYAEKEGVDPEVRHIANSPATLTLPETHFDLVRTG
Gst  THFATADEVNTDYFSYQYTRFLHMLEWLPS...RPPLVHCANSAASLRFPDRTFNMVRFG
```

Sco   α10   TTT   η2   β10   β11   TT   η3   β12

```
      240       250       260       270       280       290
Sco  IAMYGVSPSPEIGTPADFGLRPVMTLAASLALVKQVPGGHGVSYGHHYTTPGETTLGLVP
Sla  LAVYGVSPSPELGTPAQLGLRPAMTLRASLALVKTVPAGHGVSYGHHYVTESETHLALVP
Gst  IAMYGLAPSPGIKPLLPYPLKEAFSLHSRIVHVKKLQPGEKVSYGATYTAQTEEWIGTIP
```

Sco   η4   η5   β13   β14   β15   TT   TT   β16   TT

```
      300       310       320       330       340       350
Sco  LGYADGIPRHASSSGPVLVDGKWRTVAGRIAMDQFVVDLGGDRPEPGAEAVLFGPGDRGE
Sla  AGYADGIPRNASGRGPVLVAGKIRRAAGRIAMDQFVVDLGEDLAEAGDEAVILGDAERGE
Gst  IGYADGWLRRLQ.HFHVLVDGQKAPIVGRICMDQCMIRLPGPLP.VGTKVTLIGRQGDEV
```

Sco   α11   α12   TT   β17

```
      360       370       380       390
Sco  PTAEDWAQAAGTIAYEIVTRIGSRVPRVYVN.................E
Sla  PTAEDWAQAAHTIAYEIVTRIGGRVPRVYLG.................G
Gst  ISIDDVARHLETINYEVPCTISYRVPRIFFRHKRIMEVRNAIGAGESSA
```

Figure 3

A

B

Alpha-helixes
Beta-strands
Loop regions

Figure 4